HNPS Advances in Nuclear Physics

Vol 12 (2003)

HNPS2003

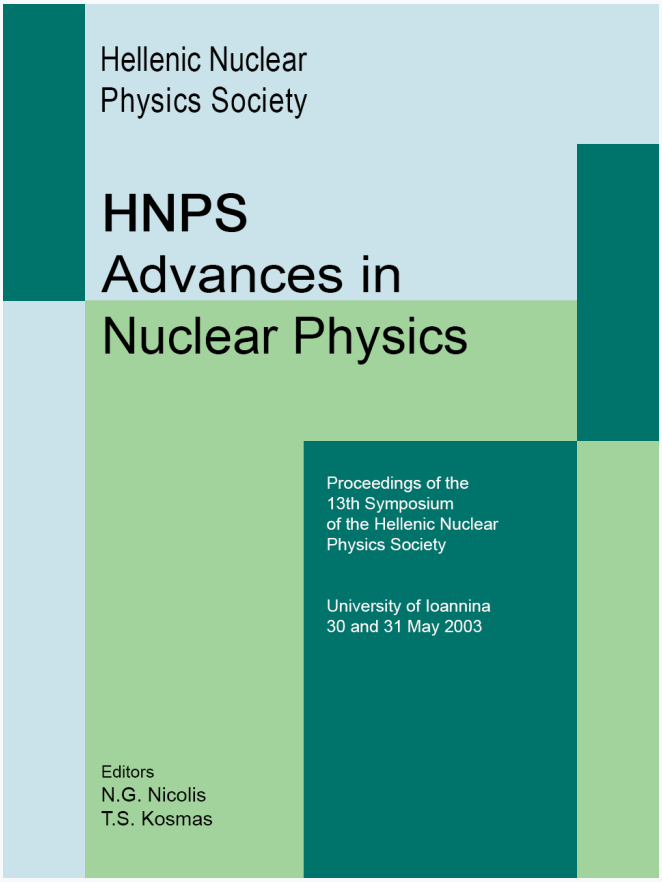

Development of a Monte-Carlo Evaporation Code for Multiple-Fragment Emission

N. G. Nicolis

doi: 10.12681/hnps.3353

HNPS Advances in Nuclear Physics vol. 12, pp. 136-145 (2003)
HNPS2003
doi:10.12681/hnps.3353

Development of a Monte-Carlo evaporation code for multiple-fragment emission

N.G. Nicolis

Department of Physics, University of Ioannina, Ioannina 45110, Greece

Abstract

An extended Hauser-Feshbach approach has been employed in a multi-step Monte-Carlo evaporation code designed to study the de-excitation of highly excited compound nuclei. The code is intended to account for emission of light particles (°, n, $^{1;2;3}$H, ^{3} i ^{6}He) and intermediate mass fragments in their ground and excited states (particle-bound or unbound). As a study case, we consider the decay of the compound nucleus ^{120}Te$^{¤}$ at excitation energy 100, 200 and 300 MeV. First chance decay widths are compared with treatments based on the Weisskopf and the s-wave approximation. Preliminary calculations are compared with experimental isotopic yields of intermediate mass fragments emitted in E/A = 50 MeV ^{4}He + $^{116;124}$Sn ! $^{120;128}$Te$^{¤}$ reactions.

1 Introduction

Statistical models of nuclear reactions play an instrumental role in the analysis and interpretation of heavy-ion reaction experiments. They can be used to verify the mechanism of a fusion-evaporation reaction, to aid in the determination of angular momenta and to search for non-statistical e¤ects at high excitation energies and angular momenta. Di¤erent types of statistical model codes have been developed, giving emphasis in the compound nucleus decay by neutron, proton, alpha and °-ray emission, which represent the dominant decay channels[1].

The need to describe rare emissions of intermediate mass fragments (IMF) with Z ¸ 3 from equilibrated compound nuclei has led to further developments in statistical model codes. Based on the Hauser-Feshbach formalism, Gomez del Campo has developed the code BUSCO [2]. BUSCO provides a deterministic calculation of cross sections of IMFs emitted in their ground and excited states (particle bound or unbound). Such a calculation is limited

in the …rst steps of the compound nucleus decay. Multi-step calculations allowing for IMF and evaporation residue cooling down to their ground states by particle emission have been presented in Ref. [3], using the Weisskopf approximation. From the point of view of the Monte-Carlo approach, the code GEMINI [4] provides a multi-step description of the deexcitation process. However, GEMINI uses the transition state formalism for the binary divisions and the Hauser-Feshbach formalism for the emission of light particles.

2 The MECO code

The need for multi-step calculations within the Hauser-Feshbach approach has led us to the development of the Monte-Carlo evaporation code MECO (Multiple-fragment Evaporation COde). MECO operates in two distinct modes. The …rst one allows a deterministic …rst chance calculation, and the second one, a complete multi-step Monte-Carlo calculation. In the following, we describe calculations of decay widths performed with various options of the code. We also present results of preliminary calculations of IMF cross sections in heavy-ion reactions assumed to proceed through the compound nucleus stage. For the purpose of our comparisons, we examine …rst-chance emissions. We consider emission of IMFs in their ground states. Furthermore, we use liquid drop model masses with shell corrections set to zero, a reasonable assumption for the excitation energy range of the present study.

2.1 Method of calculation

The Hauser-Feshbach decay width for emission of a fragment with kinetic energy ε is calculated as [5]

$$\Gamma^{HF}(\varepsilon) = \frac{1}{2\pi\hbar\rho(E^*,J)} \sum_{\ell=0}^{\infty} T_\ell(\varepsilon) \sum_{S=|J_i-\ell|}^{J_i+\ell} \sum_{j=|J_i-i_b|}^{J_i+i_b} \rho(E_f^*,I)$$

where $T_\ell(\varepsilon)$ is the transmission coe¢cient for the emission of a fragment with energy ε and angular momentum ℓ, and $\rho(E^*,J)$, $\rho(E_f^*,I)$ are the level densities of the parent and daughter nucleus, respectively.

Assuming that emissions do not remove angular momentum from the compound nucleus, $\rho(E_f^*,I) = \rho(E_f^*,J)$, we get

$$\Gamma^{S}(\varepsilon) = \frac{g_b}{\pi^2\hbar^2}\sigma_{inv}(\varepsilon)\frac{\rho(E_f^*,J)}{\rho(E^*,J)}$$

referred to as the s-wave approximation [6]. Here, $g_b = (2s+1)$ is the statistical weight of the emitted particle and $\sigma_{inv}(\varepsilon)$ is the inverse cross section of the process. Furthermore, if the level density varies as $\rho(E^*, J) \propto (2J+1)\rho(E - E_{rot}(J) - \Delta)$, where $E_{rot}(J)$ is the rotational energy for angular momentum J and Δ is the pairing energy, and $E_{rot}(J) = 0$, we get

$$\Gamma^W(\varepsilon) = \frac{g_b (2s+1)\sigma_{inv}(\varepsilon)}{\pi\hbar^2} \frac{\rho(E^*_f)}{\rho(E^*)}$$

This is the Weisskopf expression for the compound nucleus decay width [7]. Obviously, $\Gamma^S(\varepsilon)$ reduces to $\Gamma^W(\varepsilon)$ when $J = 0$.

2.2 The code ingredients

Nuclear level densities are calculated with the Fermi gas model joined smoothly with a constant temperature level density expression, below the neutron binding energy [8]. The level density constant is taken from the compilation of Gilbert and Cameron [8], or as $a = A/k$, where k is a constant. Furthermore, there is an option for using an excitation energy dependent level density parameter according to the phenomenological formula of Ignatyuk et al. [9].

Transmission coefficients for fragment emission are calculated in the framework of the optical model with global parameters [10]. Alternatively, barrier penetration transmission coefficients can be used with a choice of nuclear potentials [11,12] for the range of fragments with atomic numbers greater than an input value.

2.3 The Monte-Carlo procedure

The code starts with a compound nucleus (A_{CN}, Z_{CN}) at a given excitation energy E^* and angular momentum J. The initial distribution in (E^*, J) is specified according to an input option (projectile plus target or compound nucleus). For each one of the N open channels, the partial decay widths are calculated. Sampling the decay widths with random numbers yields the decay mode, fragment emission energy E^o (corresponding to the partial width Γ^o), and the residue angular momentum I. Then, the residual nuclear state (A, Z, E^*_f, I) is specified and treated as a new compound nucleus in the calculation. The procedure is iterated until further decays become inhibited. After each decay step, the emitter A, Z, E^*; E^*_{frag}, J, I, Γ^o, and N are written in an output event file. Cascade event separators are written at the end of each correlated decay sequence.

The event …le can be sorted by a separate code in order to allow comparisons with data constrained by the requirements of a particular experiment, i.e. geometry, detector thresholds, and gating conditions.

2.4 Comparison of decay widths

As a test case, we consider the deexcitation of the compound nucleus $^{120}Te^{\ast}$. Figure 1 shows the …rst chance decay widths (Γ_i^W) of fragments consisting of neutrons up to Ne isotopes calculated in the Weisskopf approximation. Three di¤erent excitation energies are shown by the dotted (100 MeV), dashed (200 MeV), and solid lines (300 MeV). In each case, Γ_i^W exhibit a diminishing trend with increasing fragment mass. As expected, the Γ_i^W values increase with excitation energy, especially for the heaviest fragments.

Figure 2 shows the angular momentum dependence of the Hauser-Feshbach decay widths (Γ_i^{HF}) for …rst chance neutron, proton, ^4He, and $^{6;7}Li$ emission from the compound nucleus $^{120}Te^{\ast}$ excited at 100, 200, and 300 MeV. For neutrons and protons, Γ^{HF} decreases slowly as the angular momentum increases. On the other hand, the decay widths of the more massive ejectiles (^4He, $^{6;7}Li$) increase slowly at low and more rapidly at high angular momentum. Emission

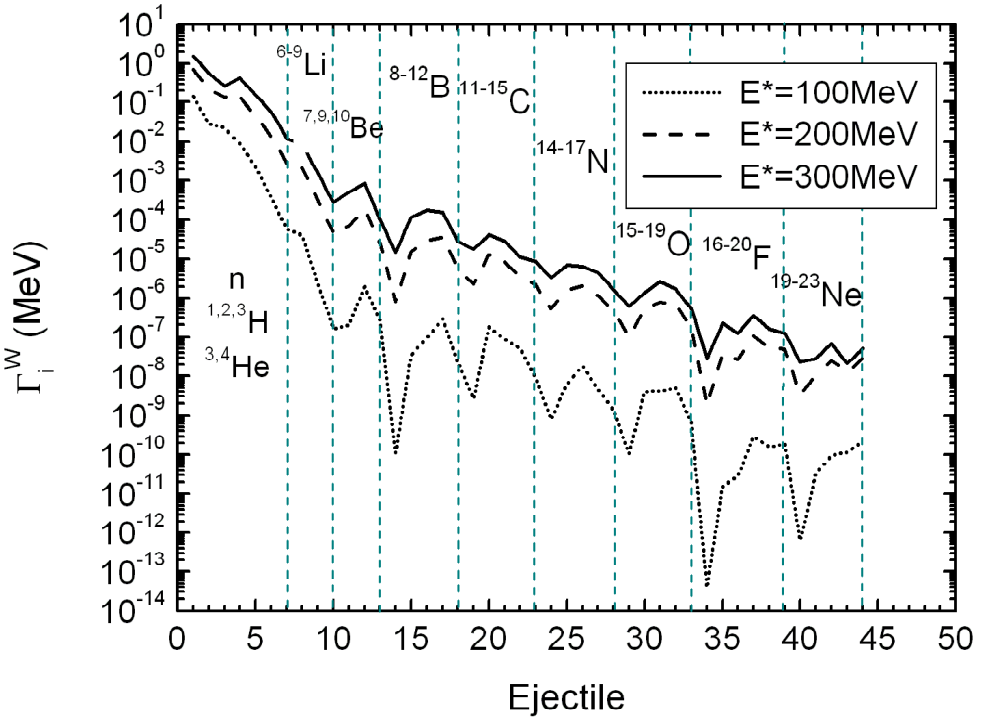

Fig. 1. First chance decay widths (in the Weisskopf approximation) of the indicated fragments emitted from the compound nucleus $^{120}Te^{\ast}$ at $E^{\ast}$ = 100, 200, and 300 MeV.

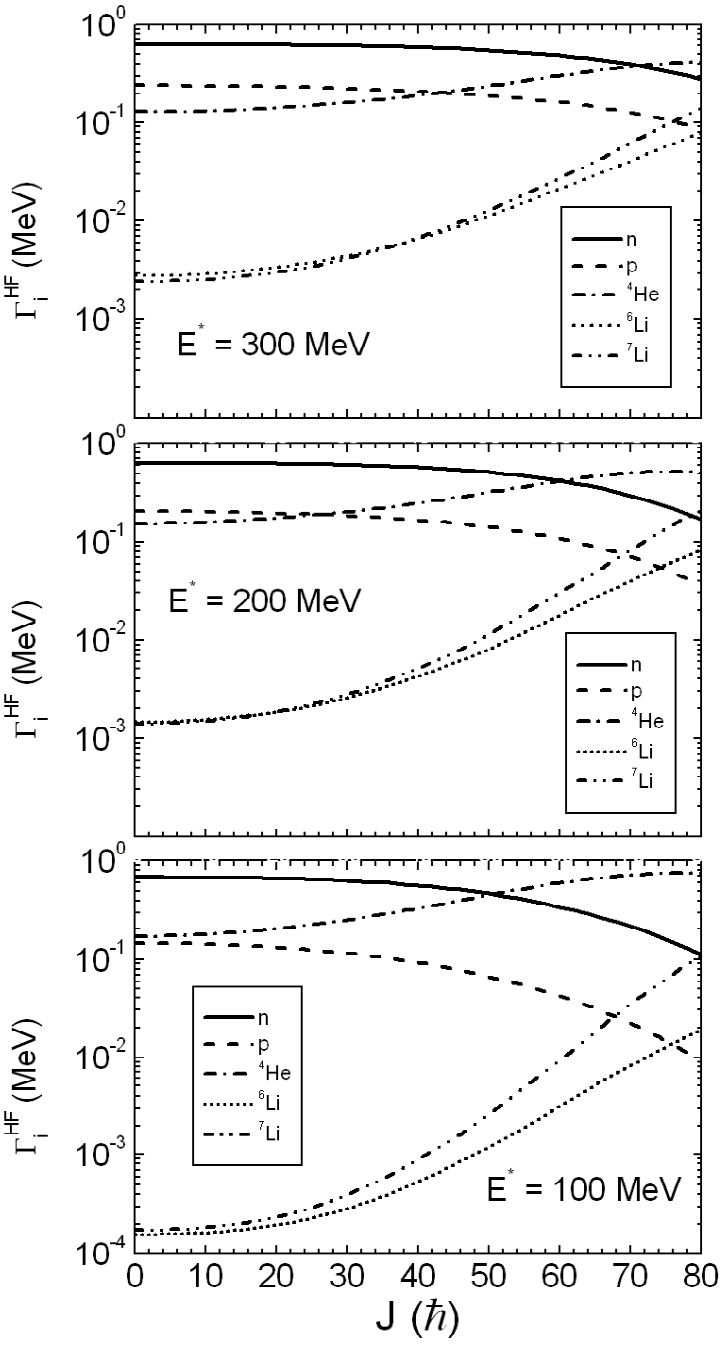

Fig. 2. Hauser-Feshbach decay widths of …rst chance emission of n, p, ^{4}He, and $^{6;7}$Li as a function of the compound nucleus ^{120}Te¤ angular momentum at E¤ = 100, 200, and 300 MeV.

of ^{7}Li dominates over ^{6}Li at low excitation energy and angular momentum. The two decay widths become comparable at high excitation energy. For all fragments, the angular momentum dependence becomes weaker at the highest excitation energy, where the yrast line plays a minor role.

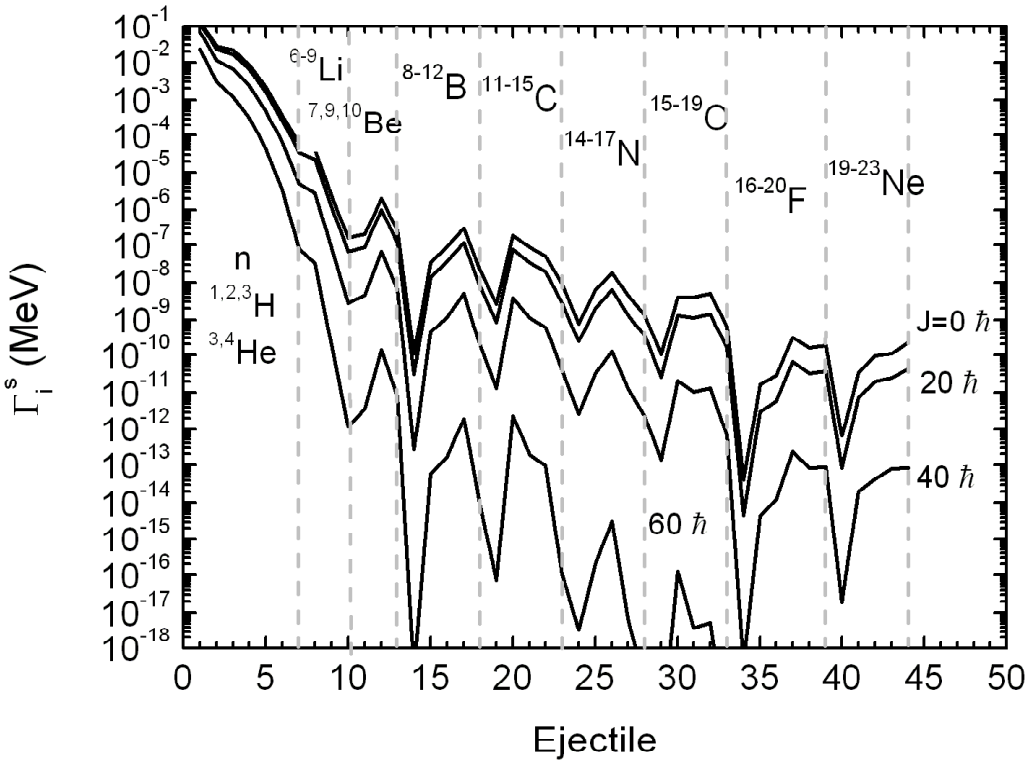

Fig. 3. First chance decay widths (in the s-wave approximation) of the indicated fragments emitted from the compound nucleus ^{120}Te¤ at E¤ = 100 MeV and J = 0;20;40, and 60ħ.

In the s-wave approximation, fragment emission does not remove angular momentum from the emitting nucleus. The presence of the yrast line is taken into account as a reduction of the e¤ective excitation energy available for decay, by the appropriate rotational energy. As a result, the decay widths at a given initial excitation energy decrease with angular momentum. This is illustrated in Fig. 3.

Figure 4 shows …rst chance decay widths for n, p, ^{4}He, ^{6}Li, and ^{12}C emitted from the compound nucleus ^{120}Te¤ as a function of the excitation energy, at the indicated values of angular momentum. In all panels, the solid curves correspond to the Hauser-Feshbach decay widths. In panels (a) and (b), the dotted lines show the results of the s-wave approximation. For J = 0ħ, there is a consistency between ¡^{s} (or ¡^{W}) and ¡^{HF} for n, p and ^{4}He emission. However, there are deviations between the two approaches as the ejectile mass increases from ^{6}Li to ^{12}C. For all fragments the two approaches deviate even more at J = 40ħ, as shown in panel (b). However, ¡^{W} provides a reasonably good approximation of ¡^{HF} at J = 40ħ, as shown in panel (c).

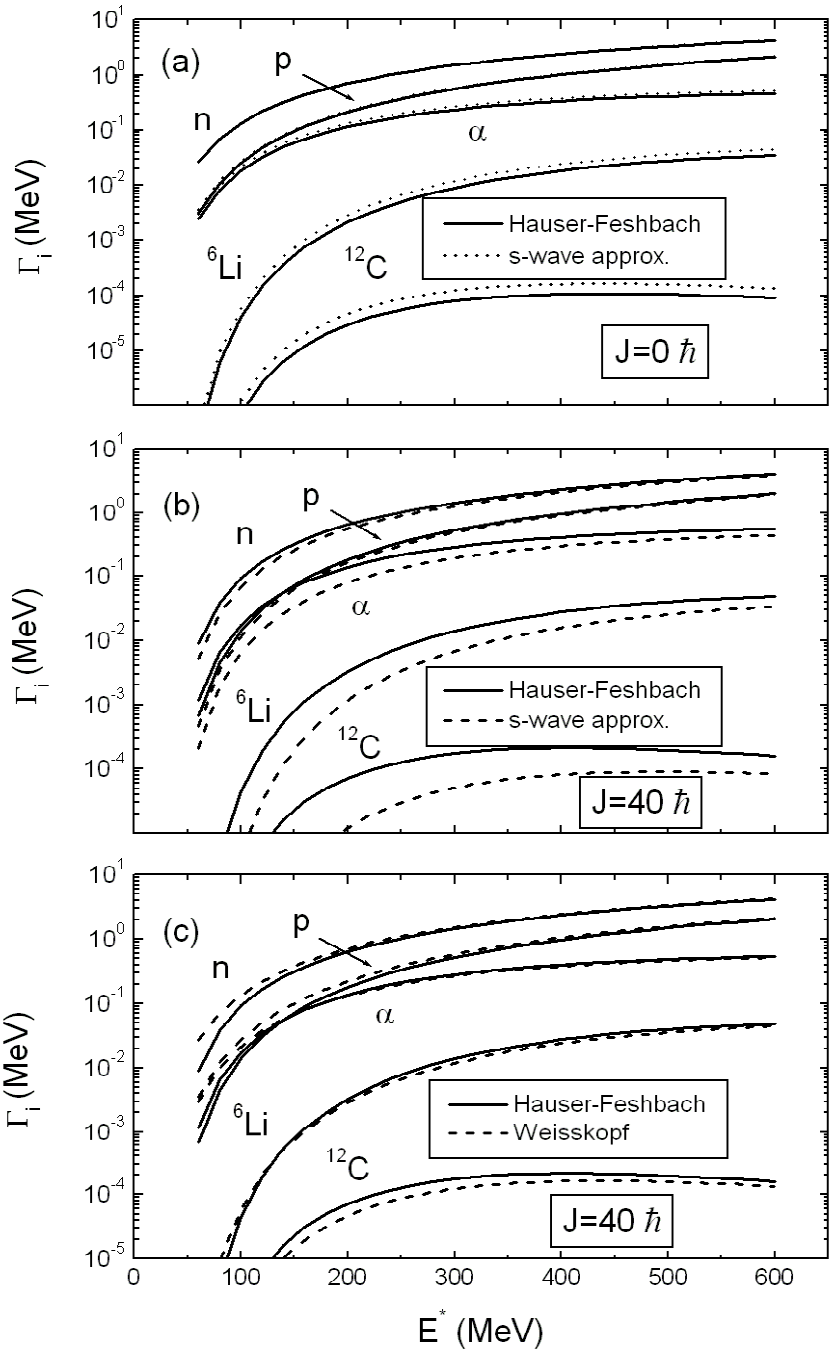

Fig. 4. First chance decay widths for n, p, ^{4}He, ^{6}Li, and ^{12}C emitted from the compound nucleus ^{120}Te¤ as a function of the excitation energy, at the indicated values of angular momentum.

The trend of decay widths with excitation energy and angular momentum can be understood from phase space considerations. Of particular interest are the deviations of the s-wave ($_i^s$) and Weisskopf ($_i^W$) approximations from the exact Hauser-Feshbach description ($_i^{HF}$). The strong reduction of $_i^s$ with angular momentum (Fig. 3 and Fig. 4a,b) implies an inadequacy of

the s-wave approximation to account for IMF emission. On the other hand, the similarity between ι^{W} and ι^{HF} at 40$\hbar$ (Fig. 4c) shows that the Weisskopf approximation is reasonable even at non-zero values of the angular momentum, for this system. This is consistent with the success of this approximation in the prediction of product yields and energy spectra of high-energy, low-spin compound nucleus reactions [13].

3 Preliminary comparisons with data

As a preliminary comparison with experimental data, we consider the Li, Be, B, and C ejectile yields observed in 50 MeV/A ^{4}He + $^{116;124}$Sn reactions [14]. These yields, expressed as isotope to element ratios are shown with symbols in Figure 5. In our calculations with MECO, it was assumed that complete fusion occurs between ^{4}He and the corresponding targets. In each case, the compound nucleus spin distributions were derived from a parabolic model approximation of the real part of the optical model potential [15]. In Fig. 5, the solid histograms show the predicted isotopic ratios, in a deterministic calculation of …rst-chance emission involving ejectiles in their ground states. We

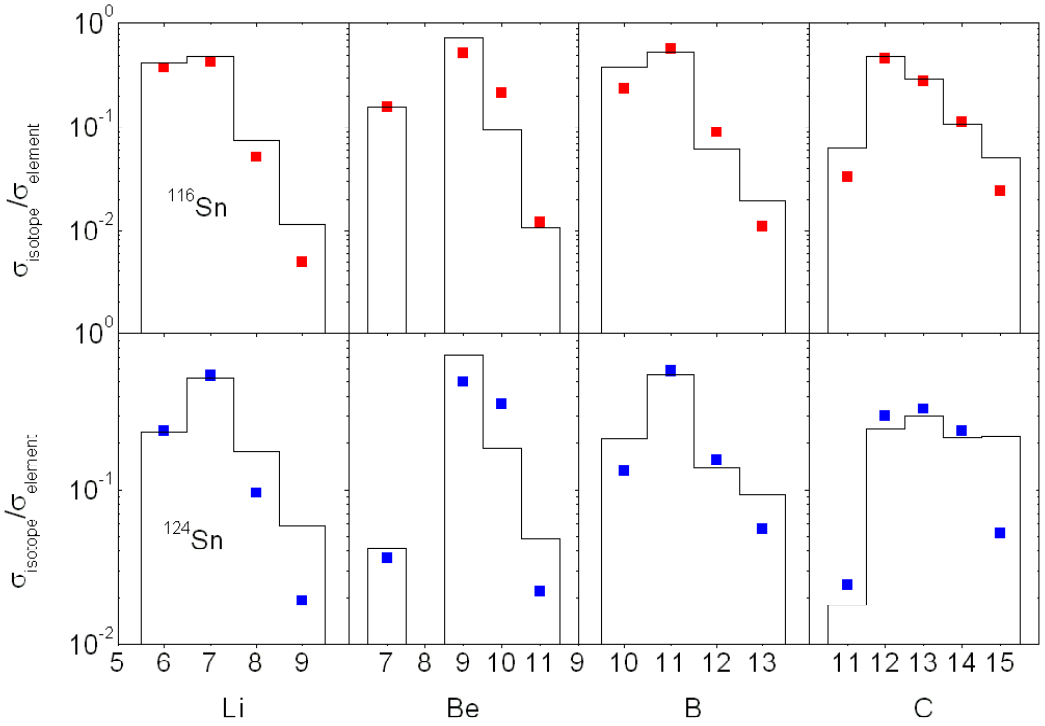

Fig. 5. Experimental isotopic distributions (symbols) for Li, Be, B, and C ejectiles in 50 MeV/A ^{4}He + $^{116;124}$Sn reactions. The solid histograms show the predicted ratios by MECO, assuming …rst-chance emission of ejectiles in their ground states.

realize a quite good agreement with the experimental data (on the general trend of the isotopic distributions and the target-isospin dependence of fragment emission) despite the fact that complete fusion has been assumed in the calculation and side-feeding from particle-unbound ejectile states has not been taken into account.

4 Summary

We presented results from the development of a multi-step Monte-Carlo evaporation code designed for the description of light-particle and intermediate mass fragment emission from highly excited compound nuclei. For simplicity and ease in comparison, we restricted ourselves in decay characteristics pertaining to …rst-chance emission.

From our comparison of …rst chance decay widths, it turns out that the s-wave approximation cannot be used as a realistic substitute of the Hauser-Feshbach treatment, even at the highest excitation energies we considered. On the other hand, the Weisskopf treatment provides a more realistic approximation at high excitation energies, despite the fact that it does not take into account the angular momentum.

Our preliminary comparison with experimental isotopic distributions in ^{4}He + $^{116;124}$Sn reactions at 50 MeV=A produced good results, despite the simplicity of these calculations. Re…nements and extensions of the code in order to treat emissions of excited fragments in the continuum are under way.

References

[1] R.G. Stokstad, in The Use of Statistical Models in Heavy-Ion Reaction Studies, Treatise on Heavy-Ion Science (Plenum Press, N.Y. 1985) Vol.3, p.83.

[2] J. Gomez del Campo, R.L. Auble, J.R. Beene, M.L. Halbert, H.J. Kim, A.D'Onofrio and J.L. Charvet, Phys. Rev. C 43, 2689(1991).

[3] M. Blann, M.G. Mustafa, G. Peilert, H. Stöcker, and W. Greiner, Phys. Rev. C44, 431(1991).

[4] R.J. Charity, M.A. McMahan, G.J. Wozniak, R.J. McDonald, L.G. Moretto, D.G. Sarantites, L.G. Sobotka, G. Guarino, A. Pantaleo, L. Fiore, A. Gobbi, and K.D. Hildenbrand, Nucl. Phys. A483, 317(1988).

[5] W. Hauser and H. Feshbach, Phys. Rev. 87, 366(1952).

[6] M. Blann and M. Beckerman, Nucleonika Vol. 23, No. 1-2/78.

[7] V. Weisskopf, Phys. Rev. 52, 295(1937); V. Weisskopf and D.H. Ewing, Phys. Rev. 57, 472(1940).

[8] A. Gilbert and A.G.W. Cameron, Can. J. Phys. 43, 1446(1965).

[9] A.V. Ignatyuk, G.N. Smirenkin, and A.S. Tishin, Sov. J. Nucl. Phys. 21, 255(1975).

[10] C.M. Perey and F.G. Perey, At. Nucl. Data Tables 17, 1(1976).

[11] J. Blocki, J. Randrup, W.S. Swiatecki, and C.F. Tsang, Ann. Phys. (N.Y.) 105, 427(1977).

[12] P.R. Christensen and A. Winther, Phys. Lett. 65B, 19(1976).

[13] H.H.K. Tang, G.R. Shinivasan, and N. Azziz, Phys. Rev. C42, 1598(1990).

[14] J. Brzychczyk, D.S. Bracken, K. Kwiatkowski, K.B. Morley, E Renshaw, and V.E. Viola, Phys. Rev. C47, 1553(1993).

[15] J.R. Huizenga and G. Igo, Nucl. Phys. 29, 462(1962).